APPLIED PHYSICS

Enhancing superconductivity in $SrTiO_3$ films with strain

Kaveh Ahadi[1]*, Luca Galletti[1], Yuntian Li[2], Salva Salmani-Rezaie[1], Wangzhou Wu[1], Susanne Stemmer[1]

The nature of superconductivity in $SrTiO_3$, the first oxide superconductor to be discovered, remains a subject of intense debate several decades after its discovery. $SrTiO_3$ is also an incipient ferroelectric, and several recent theoretical studies have suggested that the two properties may be linked. To investigate whether such a connection exists, we grew strained, epitaxial $SrTiO_3$ films, which are known to undergo a ferroelectric transition. We show that, for a range of carrier densities, the superconducting transition temperature is enhanced by up to a factor of two compared to unstrained films grown under the same conditions. Moreover, for these films, superconductivity emerges from a resistive state. We discuss the localization behavior in the context of proximity to ferroelectricity. The results point to new opportunities to enhance superconducting transition temperatures in oxide materials.

INTRODUCTION

Although $SrTiO_3$ was the first oxide superconductor to be discovered (*1*), the nature of its superconducting state has been a longstanding subject of debate in the literature (*2*–*10*), reflecting in many ways the elusiveness of other families of superconductors, such as the cuprates. A striking feature is that superconductivity already appears at very low carrier densities (*2*, *11*), when the Fermi temperature is lower than the Debye temperature, which is at odds with the Bardeen-Cooper-Schrieffer (BCS) theory. Bulk, undoped $SrTiO_3$ is an incipient ferroelectric for which quantum fluctuations suppress a low-temperature transition to a ferroelectric ground state at the lowest temperatures (*12*, *13*). Several recent theoretical proposals have suggested that a connection between the ferroelectric and superconducting properties exists (*14*–*17*), providing strong motivation for developing experimental approaches that search for such a link.

The complex relationship between metallicity and ferroelectricity is one of the main challenges in experimental tests of the role of (incipient) ferroelectricity in the superconducting pairing mechanism of $SrTiO_3$. In particular, free carriers, needed for superconductivity, and ferroelectricity do not easily coexist. For example, sufficiently large concentrations of mobile carriers can screen the splitting of the transverse and longitudinal optical phonon modes (*18*, *19*), which is essential for ferroelectricity in materials such as $SrTiO_3$ (*20*). Furthermore, conducting samples cannot sustain sufficiently large electric fields that are needed to switch a ferroelectric polarization. Thus, although there are no fundamental reasons why the two properties cannot coexist (*21*), practically, they are difficult to obtain within a homogeneous material.

Despite these challenges, several recent experiments have reported on the superconductivity of $SrTiO_3$ crystals that were tuned toward ferroelectricity by using approaches that were previously known (*22*–*24*) to stabilize ferroelectricity in insulating $SrTiO_3$. In particular, oxygen isotope doping (*25*) and alloying with Ca (*26*) were found to result in modest changes in T_C (superconducting transition temperatures) of doped single crystals.

Epitaxial coherency strains are well known to stabilize ferroelectricity in $SrTiO_3$ films (*27*–*30*). Films under different epitaxial strains thus offer an attractive platform to compare the superconducting properties of films poised to undergo a ferroelectric transition with those that remain paraelectric. Here, we show that doped, compressively

[1]Materials Department, University of California, Santa Barbara, Santa Barbara, CA 93106-5050, USA. [2]Department of Physics, University of California, Santa Barbara, Santa Barbara, CA 93106-5050, USA.
*Corresponding author. Email: kahadi@mrl.ucsb.edu

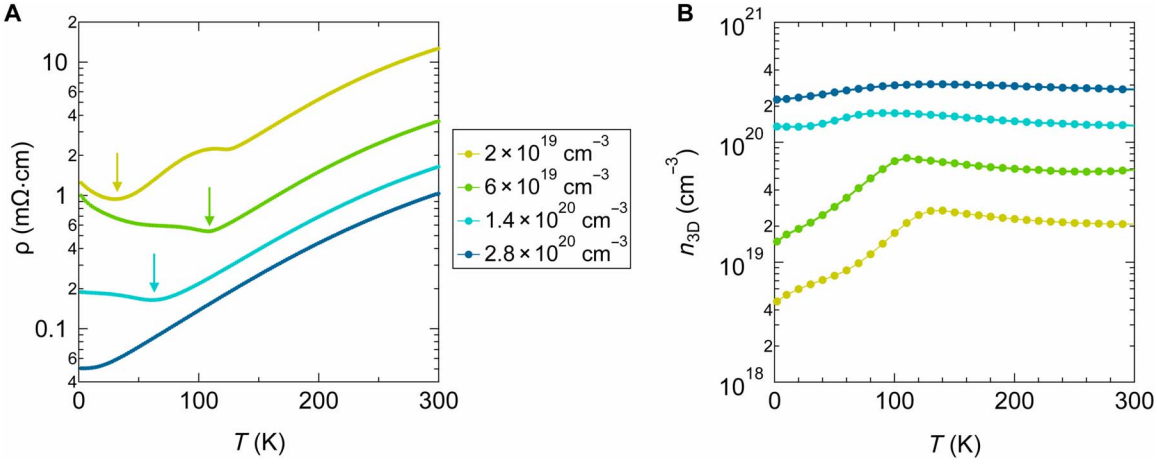

Fig. 1. Transport properties in the normal state. (**A**) Resistivity as a function of temperature (*T*) for compressively strained Sm-doped $SrTiO_3$ on LSAT substrates with different carrier densities (the legend states the carrier densities at 300 K). Upturns in the resistivity are indicated by arrows. (**B**) Hall carrier densities (n_{3D}) as a function of temperature. Lines are a guide for the eye.

strained $SrTiO_3$ films exhibit T_C values that are enhanced by a factor of two compared to unstrained films. Moreover, films with enhanced T_C exhibit a pronounced upturn in the normal state resistivity with decreasing temperature, which is highly unusual. In contrast, films with higher carrier densities remain metallic and do not exhibit enhanced T_C, although they are strained by the same amount. We discuss the implications of the results with regard to the connection between superconductivity and (incipient) ferroelectricity in $SrTiO_3$.

RESULTS

Electrical measurements were carried out on epitaxial $SrTiO_3$ films, which were grown on (001) LSAT [$(LaAlO_3)_{0.3}(Sr_2AlTaO_6)_{0.7}$] and $SrTiO_3$ substrates using a hybrid molecular beam epitaxy (MBE) technique (*31*, *32*). The films were doped with different amounts of Sm^{+3} to obtain a range of carrier densities.

Figure 1A shows the resistivities (ρ) of strained Sm:$SrTiO_3$ films grown on LSAT with different carrier densities, measured between

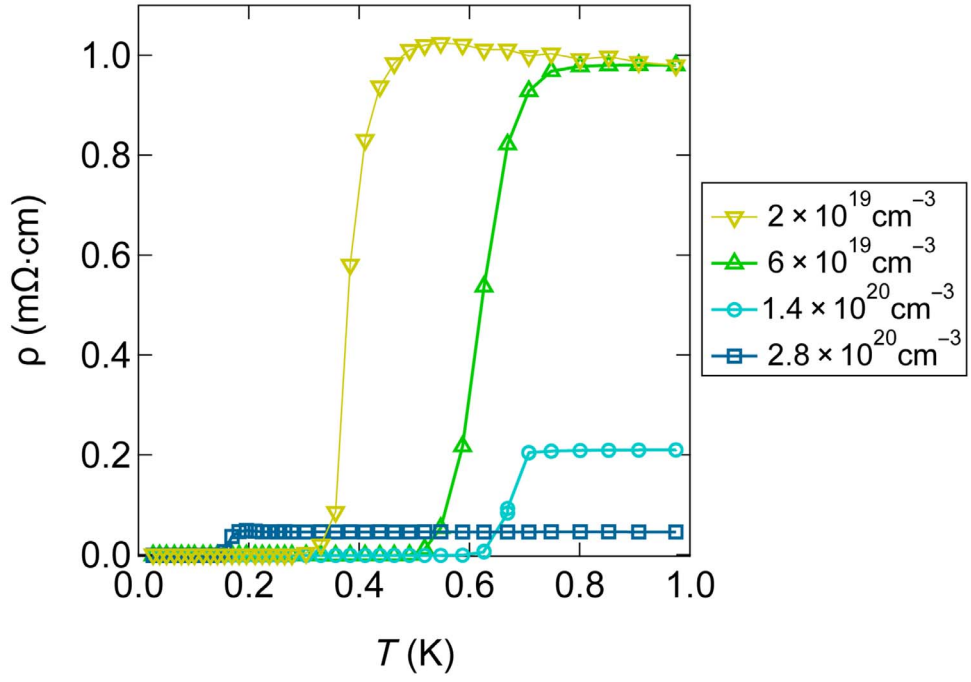

Fig. 2. Superconducting transitions for strained Sm-doped $SrTiO_3$ films with different carrier densities. The resistivity as a function of temperature between 1 K and 10 mK without an applied magnetic field is shown. The legend indicates the Hall carrier densities measured at 300 K. Lines are a guide for the eye.

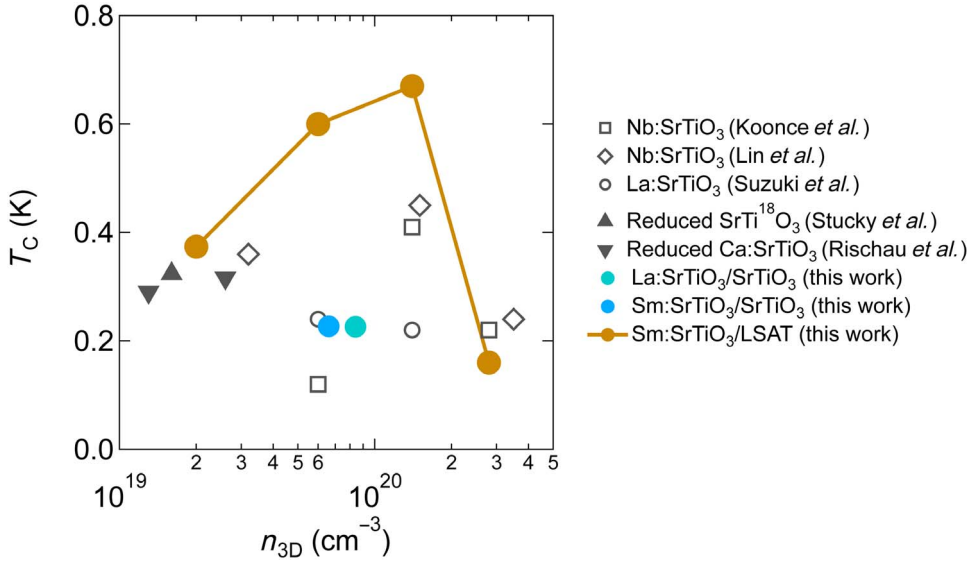

Fig. 3. Comparison of T_C of strained and unstrained $SrTiO_3$. T_C values of strained and unstrained La- and Sm-doped $SrTiO_3$ films with different carrier densities grown on LSAT and $SrTiO_3$ substrates, respectively (filled circles), are shown. T_C values of $SrTiO_3$ crystals taken from the literature are also shown, some of which were tuned toward a ferroelectric transition (triangles). Literature data are from Lin *et al.* (*11*), Stucky *et al.* (*25*), Rischau *et al.* (*26*), Koonce *et al.* (*33*), and Suzuki *et al.* (*34*). Lines are a guide for the eye.

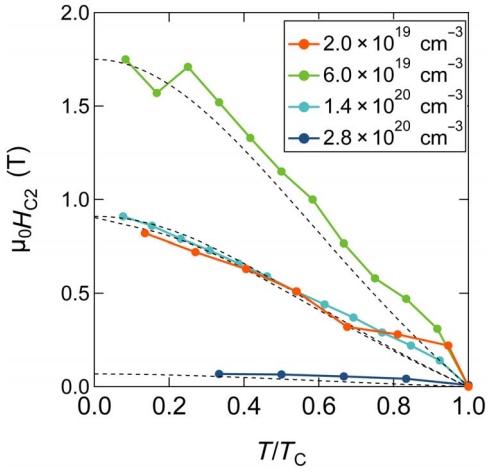

Fig. 4. Dependence of the upper critical field H_{C2} at different temperatures. The dashed lines are fits to the data (see text for details).

300 and 2 K. Here, the resistivities were determined from the sheet resistance and film thickness (200 nm) measured by cross-sectional transmission electron microscopy. The highest doped film (n_{3D} = 2.8×10^{20} cm^{-3} at 300 K, where n_{3D} is the carrier density determined from Hall measurements) shows metallic behavior, $\frac{d\rho}{dT} > 0$, down to 1.8 K. In contrast, lower doped films ($n_{3D} = 2 \times 10^{19}$, 6×10^{19}, and 1.4×10^{20} cm^{-3}) exhibit a crossover to $\frac{d\rho}{dT} < 0$ upon lowering the temperature. The transition temperatures, defined as $\frac{d\rho}{dT} = 0$, for films with $n_{3D} = 6 \times 10^{19}$ and 1.4×10^{20} cm^{-3} are ~110 and ~60 K, respectively (see arrows). The lowest doped film with $n_{3D} = 2 \times 10^{19}$ cm^{-3} not only demonstrates an upturn in resistivity at low temperatures but also shows a more complicated temperature dependence. All films exhibit an abrupt decrease in the Hall carrier density upon lowering the temperature (Fig. 1B). Roughly the same mobile carrier density (4×10^{19} to 7×10^{19} cm^{-3}) is lost in all films.

Figure 2 shows ρ between 1 K and 10 mK. All films become superconducting at low temperatures. Taking T_C as the temperature for which ρ corresponds to $\frac{\rho_n}{e}$, where ρ_n is the normal state value and e is Euler's number, the values for T_C are 0.37, 0.60, 0.67, and 0.16 K for films with $n_{3D} = 2 \times 10^{19}$, 6×10^{19}, 1.4×10^{20}, and 2.8×10^{20} cm^{-3}, respectively.

Figure 3 compares the T_C values for the films shown in Fig. 2 with those of other $SrTiO_3$ samples with similar carrier densities reported in the literature, including $SrTiO_3$ crystals that were tuned toward ferroelectricity using the approaches mentioned in the Introduction (*11*, *25*, *26*, *33*, *34*). The T_C of the Sm:$SrTiO_3$ film with the highest doping density, which remains metallic, is comparable to previous reports. In contrast, films with lower doping densities have a substantially increased T_C, which reaches almost a factor of two near the peak of the superconducting dome ("optimal doping"). Thus, the enhancement of T_C is seen for underdoped and optimally doped films but not on the overdoped side of the superconducting dome of $SrTiO_3$. For direct comparison with unstrained films grown by the same MBE method and T_C defined in the same way, Fig. 3 also shows T_C of unstrained Sm- and La-doped $SrTiO_3$ thin films grown on $SrTiO_3$ substrates, which show T_C similar to La-doped $SrTiO_3$ crystals reported in the literature (*34*). All samples shown in Fig. 3, except for the three lower doped films on LSAT, which have enhanced T_C, exhibit metallic behavior.

Figure 4 shows the superconducting upper critical magnetic field, H_{C2}, as a function of temperature. Data follow the relation $H_{C2} = H_{C2}(0)\frac{1-t^2}{1+t^2}$, where $t = T/T_C$, which is shown as dashed lines, similar to the behavior observed in La-doped films (*35*). The values of H_{C2} (i.e., 1.75 T at 50 mK for the film with $n_{3D} = 6 \times 10^{19}$ cm^{-3}) are comparable with those reported for La-doped $SrTiO_3$ films (*35*). Table 1 lists quantities derived from the data, including the values for the BCS superconducting gap, $\Delta = 1.75\, k_B T_C$, where k_B is Boltzmann's constant, and the superconducting coherence length, $\xi_0 = \sqrt{\phi_0/2\pi H_{C2}}$, where ϕ_0 is the magnetic quantum flux. Here, films with $n_{3D} = 2 \times 10^{19}$ and 1.4×10^{20} cm^{-3}, despite having different critical temperatures, show relatively similar H_{C2} at low temperatures. Thus, T_C peaks near $n_{3D} = 1.4 \times 10^{20}$ cm^{-3}, while H_{C2} peaks near $n_{3D} = 6 \times 10^{19}$ cm^{-3}. The behavior of H_{C2} might be related to the multiband nature of this superconductor (*36*) and requires further investigations beyond the scope of the present study.

Table 1. Values for T_C, H_{C2}, Δ, and ξ for Sm-doped $SrTiO_3$ films on LSAT with different carrier densities.

n_{3D} at 300 K (cm^{-3})	T_C (K)	H_{C2} at 50 mK (T)	Δ (μeV)	ξ (nm)
2×10^{19}	0.37	0.83	56	18
6×10^{19}	0.6	1.75	90	14
1.4×10^{20}	0.67	0.91	100	19
2.8×10^{20}	0.16	0.07	20	67

DISCUSSION

To briefly summarize the results, our main findings are as follows: (i) There is an enhancement in T_C of compressively strained $SrTiO_3$ films up to a factor of two, and (ii) the increase in T_C depends on the carrier density and (iii) it is connected to the presence of a crossover in the resistivity in the normal state to $\frac{d\rho}{dT} < 0$ at low temperatures.

The first important conclusion from these results is that the increase in T_C is caused not simply by the epitaxial strain, such as strain-induced modification of phonon modes. If this were the case, then all films, independent of their carrier density, should exhibit enhanced T_C, because they are all under the same epitaxial film strain. Instead, the carrier density dependence of the enhancement in T_C and the resistivity upturn point to a direct connection between a (proximal) ferroelectric state and the modified superconducting properties.

As mentioned above, $SrTiO_3$ films grown on LSAT substrates are known to transition to a ferroelectric state as a result of the epitaxial coherency strain (*27*–*30*). Even $SrTiO_3$ films containing substantial amounts of carriers (on the order of 10^{19} cm^{-3}) were found to undergo a ferroelectric transition around 140 K (*29*). Thus, the films in the present study are, at minimum, in proximity to a ferroelectric transition.

Beyond this, the observed crossover in the temperature dependence of the resistivity also hints at the emerging ferroelectric or polar nature of the films. The behavior is in marked contrast to unstrained $SrTiO_3$ films grown on $SrTiO_3$ [Fig. 3; see also (*37*) for more data] or bulk crystals of $SrTiO_3$ (*38*), which remain metallic even with orders of magnitude lower carrier densities. The reason is the high dielectric constant of $SrTiO_3$. The Mott criterion (*39*) for metallic behavior, $n^{1/3} a_B \approx 0.25$, where a_B is the Bohr radius, is thus easily exceeded, even if we assume a substantially reduced dielectric constant (~1000), which is more typical for ferroelectric $SrTiO_3$ (*29*). While carrier localization can be caused by

disorder or traps, unstrained films with similar dopant densities and disorder remain metallic. Screening of a polar charge is a reasonable explanation for the observed localization of a fixed amount of the mobile charge density (Fig. 1B). Remotely doped ferroelectric $BaTiO_3$ films undergo a transition that is very similar to the one observed here (*40*). In contrast, T_C is not increased at higher carrier densities on the overdoped side of the superconducting dome, which remains metallic. At high carrier densities, we expect the long-range interactions needed for ferroelectricity to be screened (*20*). While there is currently no agreement in the literature as to the pair-breaking mechanism that causes T_C to decrease on the overdoped side, it is expected to play a role here as well.

In summary, our experimental results, especially the carrier density dependence of the observed T_C enhancement, should be of interest for testing the different theoretical models that have been proposed in the literature that relate superconductivity in $SrTiO_3$ to a (proximal) ferroelectric state (*14*–*17*). Independent of the precise mechanism, the results point to opportunities to enhance T_C by searching for superconducting oxides that are in proximity to ferroelectricity. It would also be interesting to explore whether similar enhancement could be obtained in superconducting/ferroelectric composite structures.

Last, we would like to note that, during the preparation of this article, we became aware of a recent report of increased T_C in $SrTiO_3$ crystals under uniaxial tensile strain (*41*). The increase in T_C was attributed to a strain-induced modification of phonon modes, suggesting that other promising approaches to enhance T_C exist for $SrTiO_3$.

MATERIALS AND METHODS

Epitaxial $SrTiO_3$ films, which were doped with Sm^{+3}, were grown by a hybrid MBE technique described elsewhere (*31*, *32*). The LSAT substrate temperature was 900°C (thermocouple reading), and the growth rate was ~130 nm/hour. The carrier density scaled with the Sm flux during growth, consistent with all Sm dopants acting as donors (+3 formal valence state). The lattice mismatch results in compressive in-plane film strains (~1%), and lightly doped films are known to show a ferroelectric transition at ~140 K on this substrate (*29*). The film thickness was ~200 nm. This thickness is below the critical thickness of $SrTiO_3$ on LSAT (*42*) while being sufficiently thick to avoid substantial carrier depletion from the well-known surface depletion of $SrTiO_3$ (*43*). A combination of high-resolution x-ray diffraction (see fig. S1) and reflection high-energy electron diffraction oscillations was used to calibrate the film thickness. Laue thickness fringes were visible in x-ray diffraction and confirmed the film thickness. Reciprocal space mapping (see fig. S2) was carried out around the 113 reflection of $SrTiO_3$ and used to determine the in- and out-of-plane lattice parameters of the film and to confirm that the films remained coherently strained to the LSAT. Cross-sectional high-angle annular dark-field (HAADF) imaging in scanning transmission electron microscopy (STEM) was also used to determine the film thickness and structural quality (fig. S3). We also investigated unstrained Sm-doped $SrTiO_3$ and La-doped $SrTiO_3$ films on (001) $SrTiO_3$ substrates grown under the same conditions.

Temperature-dependent measurements of the longitudinal and Hall resistances were carried out using a Quantum Design Physical Property Measurement System. The Hall carrier densities extracted from the Hall measurements, $n_{3D} = -1/(teR_H)$, where t is the thickness of the $Sm_xSr_{1-x}TiO_3$ thin film, e is the electron charge, and R_H is the Hall coefficient $R_H = dR_{xy}/dB$, were extracted from linear fits to the transverse resistance $R_H(B)$ with the magnetic field (B). Magnetotransport measurements below 1 K were carried out in a dilution refrigerator (Triton, Oxford Instruments Group). Transport measurements were carried out in van der Pauw geometry with square-shaped samples (5 mm × 5 mm). Ohmic contacts (40-nm Ti/400-nm Au) were deposited on the sample corners (<0.5 mm × 0.5 mm) through a shadow mask using an electron beam evaporation. The superconductivity measurements were carried out using a lock-in amplifier (SR830, Stanford Research Systems) in AC mode with an excitation current of 1 μA and a frequency of 33.33 Hz. The critical field was obtained from measuring the longitudinal resistance while sweeping an out-of-plane magnetic field at different temperatures (see fig. S4).

SUPPLEMENTARY MATERIALS

Supplementary material for this article is available at http://advances.sciencemag.org/cgi/content/full/5/4/eaaw0120/DC1

Fig. S1. 2θ-ω scan of a $SrTiO_3$ film on LSAT near the 001 reflections.
Fig. S2. RSM of a $SrTiO_3$/LSAT heterostructure around the 113 reflection.
Fig. S3. Cross-sectional HAADF-STEM images.
Fig. S4. Magnetic field dependence of the superconducting transition.
Fig. S5. Superconducting transitions for Sm- and La-doped $SrTiO_3$ films grown on $SrTiO_3$ substrates.
Fig. S6. Resistivity as a function of temperature for Sm-doped $SrTiO_3$ films grown on $SrTiO_3$ substrates.

REFERENCES AND NOTES

1. J. F. Schooley, W. R. Hosler, M. L. Cohen, Superconductivity in semiconducting $SrTiO_3$. *Phys. Rev. Lett.* **12**, 474–475 (1964).
2. J. Appel, Soft-mode superconductivity in $SrTiO_{3-x}$. *Phys. Rev.* **180**, 508–516 (1969).
3. G. Binnig, A. Baratoff, H. E. Hoenig, J. G. Bednorz, Two-band superconductivity in Nb-doped $SrTiO_3$. *Phys. Rev. Lett.* **45**, 1352–1355 (1980).
4. Y. Takada, Theory of superconductivity in polar semiconductors and its application to N-type semiconducting $SrTiO_3$. *J. Phys. Soc. Jpn.* **49**, 1267–1275 (1980).
5. A. Baratoff, G. Binnig, Mechanism of superconductivity in $SrTiO_3$. *Phys. B & C* **108**, 1335–1336 (1981).
6. D. van der Marel, J. L. M. van Mechelen, I. I. Mazin, Common Fermi-liquid origin of T^2 resistivity and superconductivity in *n*-type $SrTiO_3$. *Phys. Rev. B* **84**, 205111 (2011).
7. L. P. Gor'kov, Phonon mechanism in the most dilute superconductor *n*-type $SrTiO_3$. *Proc. Natl. Acad. Sci. U.S.A.* **113**, 4646–4651 (2016).
8. J. Ruhman, P. A. Lee, Superconductivity at very low density: The case of strontium titanate. *Phys. Rev. B* **94**, 224515 (2016).
9. A. G. Swartz, H. Inoue, T. A. Merz, Y. Hikita, S. Raghu, T. P. Devereaux, S. Johnston, H. Y. Hwang, Polaronic behavior in a weak-coupling superconductor. *Proc. Natl. Acad. Sci. U.S.A.* **115**, 1475–1480 (2018).
10. M. Thiemann, M. H. Beutel, M. Dressel, N. R. Lee-Hone, D. M. Broun, E. Fillis-Tsirakis, H. Boschker, J. Mannhart, M. Scheffler, Single-gap superconductivity and dome of superfluid density in Nb-doped $SrTiO_3$. *Phys. Rev. Lett.* **120**, 237002 (2018).
11. X. Lin, Z. Zhu, B. Fauqué, K. Behnia, Fermi surface of the most dilute superconductor. *Phys. Rev. X* **3**, 021002 (2013).
12. K. A. Müller, H. Burkard, $SrTiO_3$: An intrinsic quantum paraelectric below 4 K. *Phys. Rev. B* **19**, 3593–3602 (1979).
13. W. Zhong, D. Vanderbilt, Effect of quantum fluctuations on structural phase transitions in $SrTiO_3$ and $BaTiO_3$. *Phys. Rev. B* **53**, 5047–5050 (1996).
14. J. M. Edge, Y. Kedem, U. Aschauer, N. A. Spaldin, A. V. Balatsky, Quantum critical origin of the superconducting dome in $SrTiO_3$. *Phys. Rev. Lett.* **115**, 247002 (2015).
15. S. E. Rowley, L. J. Spalek, R. P. Smith, M. P. M. Dean, M. Itoh, J. F. Scott, G. G. Lonzarich, S. S. Saxena, Ferroelectric quantum criticality. *Nat. Phys.* **10**, 367–372 (2014).
16. S. E. Rowley, C. Enderlein, J. F. de Oliveira, D. A. Tompsett, E. B. Saitovitch, S. S. Saxena, G. G. Lonzarich, Superconductivity in the vicinity of a ferroelectric quantum phase transition. arXiv:1801.08121 [cond-mat.supr-con] (24 January 2018).
17. K. Dunnett, A. Narayan, N. A. Spaldin, A. V. Balatsky, Strain and ferroelectric soft-mode induced superconductivity in strontium titanate. *Phys. Rev. B* **97**, 144506 (2018).
18. A. Mooradia, G. B. Wright, Observation of the interaction of plasmons with longitudinal optical phonons in GaAs. *Phys. Rev. Lett.* **16**, 999–1001 (1966).
19. E. F. Steigmeier, G. Harbeke, Soft phonon mode and ferroelectricity in GeTe. *Solid State Commun.* **8**, 1275–1279 (1970).
20. W. Zhong, R. D. King-Smith, D. Vanderbilt, Giant LO-TO splittings in perovskite ferroelectrics. *Phys. Rev. Lett.* **72**, 3618–3621 (1994).
21. A. Filippetti, V. Fiorentini, F. Ricci, P. Delugas, J. Iñiguez, Prediction of a native ferroelectric metal. *Nat. Commun.* **7**, 11211 (2016).

22. M. Itoh, R. Wang, Y. Inaguma, T. Yamaguchi, Y.-J. Shan, T. Nakamura, Ferroelectricity induced by oxygen isotope exchange in strontium titanate perovskite. *Phys. Rev. Lett.* **82**, 3540–3543 (1999).
23. H. Uwe, T. Sakudo, Stress-induced ferroelectricity and soft phonon modes in $SrTiO_3$. *Phys. Rev. B* **13**, 271–286 (1976).
24. J. G. Bednorz, K. A. Müller, $Sr_{1-x}Ca_x$ TiO_3: An XY quantum ferroelectric with transition to randomness. *Phys. Rev. Lett.* **52**, 2289–2292 (1984).
25. A. Stucky, G. W. Scheerer, Z. Ren, D. Jaccard, J.-M. Poumirol, C. Barreteau, E. Giannini, D. van der Marel, Isotope effect in superconducting n-doped $SrTiO_3$. *Sci. Rep.* **6**, 37582 (2016).
26. C. W. Rischau, X. Lin, C. P. Grams, D. Finck, S. Harms, J. Engelmayer, T. Lorenz, Y. Gallais, B. Fauqué, J. Hemberger, K. Behnia, A ferroelectric quantum phase transition inside the superconducting dome of $Sr_{1-x}Ca_xTiO_{3-\delta}$. *Nat. Phys.* **13**, 643–648 (2017).
27. J. H. Haeni, P. Irvin, W. Chang, R. Uecker, P. Reiche, Y. L. Li, S. Choudhury, W. Tian, M. E. Hawley, B. Craigo, A. K. Tagantsev, X. Q. Pan, S. K. Streiffer, L. Q. Chen, S. W. Kirchoefer, J. Levy, D. G. Schlom, Room-temperature ferroelectricity in strained $SrTiO_3$. *Nature* **430**, 758–761 (2004).
28. N. A. Pertsev, A. K. Tagantsev, N. Setter, Phase transitions and strain-induced ferroelectricity in $SrTiO_3$ epitaxial thin films. *Phys. Rev. B* **61**, R825–R829 (2000).
29. A. Verma, S. Raghavan, S. Stemmer, D. Jena, Ferroelectric transition in compressively strained $SrTiO_3$ thin films. *Appl. Phys. Lett.* **107**, 192908 (2015).
30. R. C. Haislmaier, R. Engel-Herbert, V. Gopalan, Stoichiometry as key to ferroelectricity in compressively strained $SrTiO_3$ films. *Appl. Phys. Lett.* **109**, 032901 (2016).
31. B. Jalan, R. Engel-Herbert, N. J. Wright, S. Stemmer, Growth of high-quality $SrTiO_3$ films using a hybrid molecular beam epitaxy approach. *J. Vac. Sci. Technol. A* **27**, 461–464 (2009).
32. J. Son, P. Moetakef, B. Jalan, O. Bierwagen, N. J. Wright, R. Engel-Herbert, S. Stemmer, Epitaxial $SrTiO_3$ films with electron mobilities exceeding 30,000 $cm^2 V^{-1} s^{-1}$. *Nat. Mater.* **9**, 482–484 (2010).
33. C. S. Koonce, M. L. Cohen, J. F. Schooley, W. R. Hosler, E. R. Pfeiffer, Superconducting transition temperatures of semiconducting $SrTiO_3$. *Phys. Rev.* **163**, 380–390 (1967).
34. H. Suzuki, H. Bando, Y. Ootuka, I. H. Inoue, T. Yamamoto, K. Takahashi, Y. Nishihara, Superconductivity in single-crystalline $Sr_{1-x}La_xTiO_3$. *J. Phys. Soc. Jpn.* **65**, 1529–1532 (1996).
35. D. Olaya, F. Pan, C. T. Rogers, J. C. Price, Superconductivity in La-doped strontium titanate thin films. *Appl. Phys. Lett.* **84**, 4020–4022 (2004).
36. X. Lin, G. Bridoux, A. Gourgout, G. Seyfarth, S. Kramer, M. Nardone, B. Fauqué, K. Behnia, Critical doping for the onset of a two-band superconducting ground state in $SrTiO_{3-\delta}$. *Phys. Rev. Lett.* **112**, 207002 (2014).
37. T. A. Cain, A. P. Kajdos, S. Stemmer, La-doped $SrTiO_3$ films with large cryogenic thermoelectric power factors. *Appl. Phys. Lett.* **102**, 182101 (2013).
38. A. Spinelli, M. A. Torija, C. Liu, C. Jan, C. Leighton, Electronic transport in doped $SrTiO_3$: Conduction mechanisms and potential applications. *Phys. Rev. B* **81**, 155110 (2010).
39. N. F. Mott, *Metal-Insulator Transitions* (Taylor & Francis, ed. 2, 1990).
40. S. Raghavan, J. Y. Zhang, O. F. Shoron, S. Stemmer, Probing the metal-insulator transition in $BaTiO_3$ by electrostatic doping. *Phys. Rev. Lett.* **117**, 037602 (2016).
41. C. Herrera, J. Cerbin, K. Dunnett, A. V. Balatsky, I. Sochnikov, arXiv:1808.03739 [cond-mat. supr-con] (11 August 2018).
42. T. Wang, K. Ganguly, P. Marshall, P. Xu, B. Jalan, Critical thickness and strain relaxation in molecular beam epitaxy-grown $SrTiO_3$ films. *Appl. Phys. Lett.* **103**, 212904 (2013).
43. A. Ohtomo, H. Y. Hwang, Surface depletion in doped $SrTiO_3$ thin films. *Appl. Phys. Lett.* **84**, 1716–1718 (2004).

Acknowledgments

Funding: This work was supported by the NSF (grant nos. 1740213 and 1729489) and a Vannevar Bush Faculty Fellowship of the Department of Defense (grant no. N00014-16-1-2814). The dilution fridge used in the measurements was funded through the Major Research Instrumentation program of the U.S. NSF (award no. DMR 1531389). This work made use of the MRL Shared Experimental Facilities, which are supported by the MRSEC Program of the U.S. NSF under award no. DMR 1720256. **Author contributions:** K.A. grew the samples and performed electrical measurements and data analysis. Y.L. and L.G. assisted with electrical measurements and analysis. S.S.-R. performed transmission electron microscopy measurements, and W.W. assisted with x-ray diffraction studies. K.A. and S.S. wrote the manuscript. **Competing interests:** The authors declare that they have no competing interests. **Data and materials availability:** All data needed to evaluate the conclusions in the paper are present in the paper and/or the Supplementary Materials. Additional data related to this paper may be requested from the authors.

Submitted 13 November 2018
Accepted 6 March 2019
Published 26 April 2019
10.1126/sciadv.aaw0120

Citation: K. Ahadi, L. Galletti, Y. Li, S. Salmani-Rezaie, W. Wu, S. Stemmer, Enhancing superconductivity in $SrTiO_3$ films with strain. *Sci. Adv.* **5**, eaaw0120 (2019).